

## CHAPTER 143

### Flow Computations nearby a Storm Surge Barrier under Construction with Two-Dimensional Numerical Models

H.E. Klatter       \*  
J.M.C. Dijkzeul   \*\*  
G. Hartsuiker     \*\*\*  
L. Bijlsma       \*\*\*\*

This paper discusses the application of two-dimensional tidal models to the hydraulic research for the storm surge barrier in the Eastern Scheldt in the Netherlands.

At the site of the barrier local energy losses dominate the flow. Three methods are discussed for dealing with these energy losses in a numerical model based on the long wave equations.

The construction of the storm surge barrier provided extensive field data for various phases of the construction of the barrier and these field data are used as a test case for the computation at methods developed. One method is preferred since it gives good agreement between computations and field data. The two-dimensional flow patterns, the discharge and the head-difference agree well.

The results of scale model tests were also available for comparison. This comparison demonstrated that depth-averaged velocities, computed by a two-dimensional numerical model, are as accurate as values obtained from a large physical scale model. Even complicated flow patterns with local energy losses and sharp velocity gradients compared well.

#### Introduction

As result of the 1953 storm flood disaster the Dutch government initiated a comprehensive construction program called the Delta Plan. Its purpose is to protect the south western part of the Netherlands against storm surges from the North Sea. In accordance with the Plan most Dutch estuaries have been closed by dams. The final, and by far the largest inlet, the Eastern Scheldt (Figure 1) will not be closed, but safety will be ensured by a storm surge barrier. Under normal weather conditions the barrier gates will be open and the tidal move-

\* Hydraulic Engineer, Hydraulic Research Division, Ministry of Transport and Public Works, P.O. Box 5044, 2600 GA Delft, The Netherlands.

\*\* Mathematician, Tidal Water Division, Ministry of Transport and Public Works, Van Alkemadelaan 400, 2597 AT, The Hague, The Netherlands.

\*\*\* Project Engineer, Delft Hydraulics Laboratory, P.O. Box 152, 8300 AD, Emmeloord, The Netherlands.

\*\*\*\* Senior Engineer, Zeeland Division, Ministry of Transport and Public Works, P.O. Box 5014, 4330 KA Middelburg, The Netherlands.

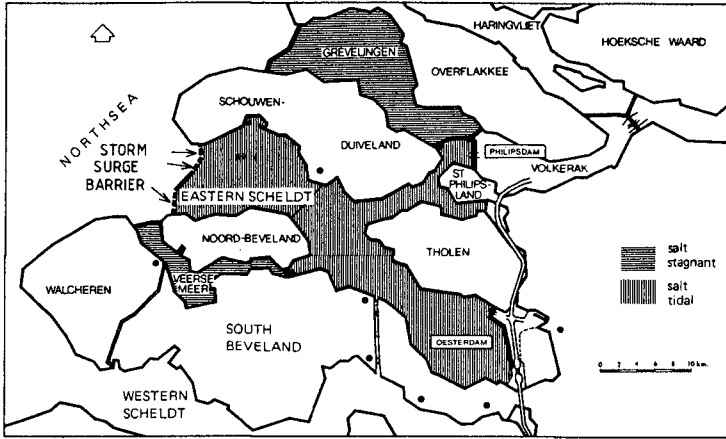
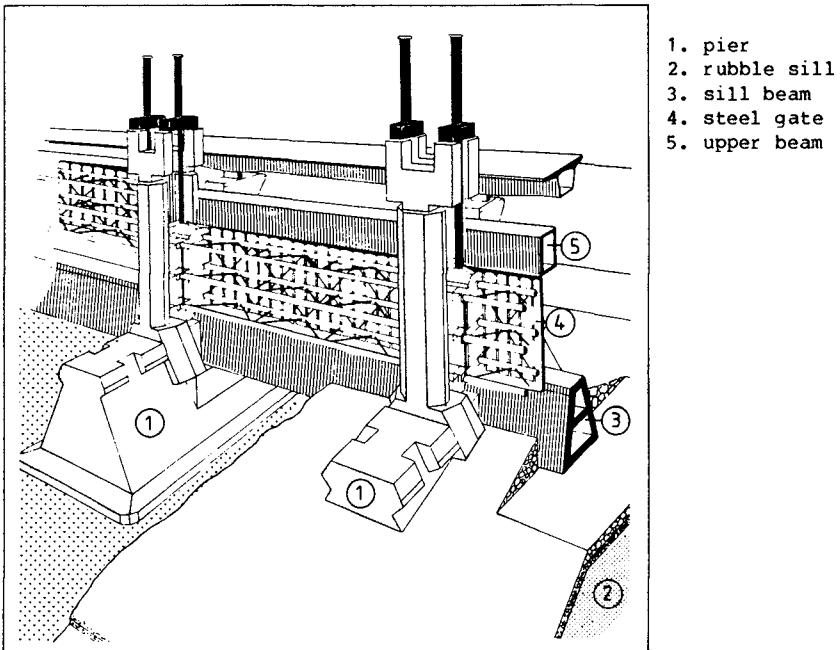


Figure 1. Location of the Storm Surge Barrier.

ment in the estuary will be maintained. This will preserve the unique-Eastern Scheldt environment. During storm surges the 62 gates of the barrier will be closed.



- 1. pier
- 2. rubble sill
- 3. sill beam
- 4. steel gate
- 5. upper beam

Figure 2. Storm Surge Barrier.

The barrier, which was completed in October 1986, has been built in the three main tidal channels. The structure comprises prefabricated piers, rubble sills, concrete sill beams and steel gates (Figure 2). Since the structural elements were to be prefabricated and positioned under open sea conditions, using specially constructed floating derricks, an extensive research program concerning the water motion in the vicinity of the barrier was needed. This research program extended over a period of 10 years, both before and during the barrier construction and was aimed at optimizing the design of the structural elements and derricks and achieving better execution management for the construction works.

At the site of the storm surge barrier the tidal range varies between 2.5 and 3.5 m. The continued reduction of the hydraulic cross-section during the barrier construction, caused increases in current velocities up to 5 m/s through the barrier, under normal tidal conditions. This paper discusses the use of two dimensional numerical models for the prediction of the depth-averaged tidal motion. These computations provide detailed information of for example:

- overall tidal motion, total discharge
- flow patterns in the mouth of the estuary, used in the prediction of morphological effects
- detailed flow patterns in the vicinity of the barrier for computing, for example, local scour near the barrier.

#### Main Features of the Numerical Solution

For the two-dimensional (horizontal) simulation of tidal motion the WAQUA program system is used. WAQUA is originally developed by the Rand Corporation, USA. In its further development it has been redesigned by the Data Processing Division of the Netherlands Department of Transport and Public Works and the Delft Hydraulics Laboratory.

WAQUA is based on a numerical solution of the two-dimensional long wave equations. These are derived under the following assumptions:

- i) vertical velocities and accelerations are negligible relative to the gravitational acceleration; in other words, hydrostatic pressure distribution is assumed (nearly parallel flow).
- ii) the water body is well-mixed vertically.

The resulting equations, containing vertically averaged velocity components, are:

$$\frac{\partial U}{\partial t} + U \frac{\partial U}{\partial x} + V \frac{\partial U}{\partial y} - fV + g \frac{\partial \zeta}{\partial x} - v_t \left( \frac{\partial^2 U}{\partial x^2} + \frac{\partial^2 U}{\partial y^2} \right) + g \frac{U(U^2+V^2)^{\frac{1}{2}}}{C^2(h+\zeta)} + X = 0 \quad (1)$$

$$\frac{\partial V}{\partial t} + U \frac{\partial V}{\partial x} + V \frac{\partial V}{\partial y} + fU + g \frac{\partial \zeta}{\partial y} - v_t \left( \frac{\partial^2 V}{\partial x^2} + \frac{\partial^2 V}{\partial y^2} \right) + g \frac{V(U^2+V^2)^{\frac{1}{2}}}{C^2(h+\zeta)} + Y = 0 \quad (2)$$

$$\frac{\partial \zeta}{\partial t} + \frac{\partial((h+\zeta)U)}{\partial x} + \frac{\partial((h+\zeta)V)}{\partial y} = 0 \quad (3)$$

where:

U = depth-averaged velocity in x direction (m/s)

$V$	= depth-averaged velocity in y direction	(m/s)
$\zeta$	= water elevation relative to the reference plane	(m)
$h$	= distance from the bottom to the reference plane	(m)
$t$	= time	(s)
$X, Y$	= external force components per unit mass	(m/s <sup>2</sup> )
$f$	= Coriolis parameter	(s <sup>-1</sup> )
$g$	= acceleration due to gravity	(m/s <sup>2</sup> )
$\nu_t$	= eddy viscosity coefficient	(m <sup>2</sup> /s)
$C$	= Chézy coefficient for bottom friction	(m <sup>1/2</sup> /s)

Equations 1, 2 and 3 are solved at discrete space increments and discrete time intervals by an implicit finite difference method (References 2,3,4). The model area is schematized by a two-dimensional grid composed of equal square cells. In addition, the system possesses a facility to simulate drying and flooding processes of the tidal flats. The eddy viscosity coefficient  $\nu_t$  is a constant, the corresponding terms taking care of lateral momentum transfer. At the site of the barrier the flow is dominated by energy losses generated by the rapid acceleration and deceleration of the flow. Local vertical velocities and accelerations are then no longer negligible and the depth-averaged equations, equations 1,2 and 3, are no longer valid. A resistance law is applied here, based on an equation of motion derived from the Bernoulli equation (accelerating flow, see Figure 3):

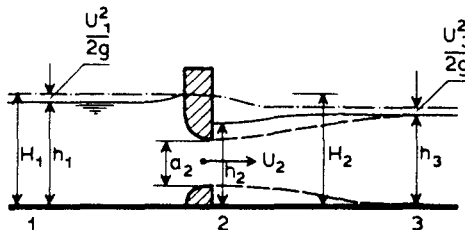


Figure 3. Flow at the Barrier Site.

$$q = a_2 \sqrt{2g(H_1 - h_2)} \quad (4)$$

where:

$q$	= discharge per unit length	(m <sup>2</sup> /s)
$a_2$	= cross section height at Section 2	(m)
$g$	= acceleration due to gravity	(m/s <sup>2</sup> )
$H_1$	= upstream energy level	(m)
$h_2$	= waterlevel at Section 2	(m)

In Equation 4, the waterlevel  $h_2$  is replaced by the downstream waterlevel  $h_3$  and a discharge coefficient,  $\mu$ , is added to compensate

for energy losses caused by the deceleration of the flow. For practical applications the upstream energy level  $H_1$  is replaced by the waterlevel  $h_1$ . The inaccuracy of this approximation is small when

$$\frac{U_1^2}{2g} \ll \frac{U_2^2}{2g}$$

$U_1$  and  $U_2$  are depth-averaged velocities at Section 1 and 2 respectively.

The resulting equation is:

$$q = \mu a_2 \sqrt{2g (h_1 - h_3)} \quad (5)$$

where:

$q$	= discharge per unit length	(m <sup>2</sup> /s)
$\mu$	= discharge coefficient	(-)
$a_2$	= cross section height at section 2	(m)
$g$	= acceleration due to gravity	(m/s <sup>2</sup> )
$h_1$	= upstream water level	(m)
$h_3$	= downstream water level	(m)

The discharge coefficient can be obtained from flume tests or from literature. Equation 5 describes a steady state type of flow. For unsteady flow this approach is not precise for the short period around slack water. For most applications this is of minor importance and can be neglected.

Three different methods introducing energy losses at the barrier site into the WAQUA program were applied:

1- Substitution of the long wave equation by a barrier equation.

At the barrier site the long wave equations, Equations 1,2 and 3, are replaced by Equation 5, creating a sort of internal boundary at the barrier site. Both sides of this boundary are coupled by Equation 5.

2- Adapted fixed roughness.

At the barrier site an adapted fixed value of the Chézy coefficient is calculated by equating the Chézy equation to Equation 5. At the barrier site equations 1, 2 and 3 are solved completely.

3- Dynamically adapted roughness

This is a mixed version of methods 1 and 2.

At the barrier site the roughness coefficient is continuously adapted so that the discharge and headloss satisfy Equation 5 for a given value of the discharge coefficient,  $\mu$ .

Thus continually a new Chézy value is calculated during the computation.

Methods 1 and 3 make it possible to use different coefficients for different flow directions and different equations for different flow conditions, such as subcritical or supercritical flow.

With Methods 1 and 3 Equation 5 is solved by an explicit method. The solution is found iteratively so that it fits in the results calculated by the implicit WAQUA scheme precisely.

### Application of Two-Dimensional Numerical Models to the Storm Surge Barrier in the Eastern Scheldt

In the case of the Eastern Scheldt it is not feasible to use one single model for all purposes. A set of models is therefore used which consists of an overall tidal model and a number of nested detail models (Figure 4).

The main function of the overall model is to provide boundary conditions for the detail models. The overall model covers the entire estuary of the Eastern Scheldt. The model has a length of 65 km and a maximum breadth of 15 km. The grid size is 400 m.

A relatively large detail model describes the mouth of the Eastern Scheldt. This model covers an area 21 km long and 10 km broad. The grid size is 100 m. The model is used to evaluate relatively large scale phenomena such as morphological changes in the tidal channels and on the tidal flats between the main channels (Reference 1).

A set of nested models is used to compute details of the flow pattern in the vicinity of the barrier. This set consists of two models with 90 m grid size and a model area equivalent to 10 x 6 km. One model contains both the northern branches of the estuary, the Hammen and the Schaar, and the other contains the south branch, the Roompot.

Three separate models each with 45 m grid size, are used for the Hammen, the Schaar and the Roompot. The area of these models is equivalent to about 3,5 x 2,5 km. The axis of the 45 m models are orientated so that one axis is parallel to the barrier.

The boundary conditions for the models are a mixture of velocity type and of waterlevel type boundary conditions.

This paper discusses the results of the small detail models, 45 m grid size, in more detail. The parameters used for the calibration of the models are:

$v_t$ ,  $C$  and  $\mu$  see Equations 1, 2, 3 and 5. Also the grid size and the timestep are important to the accuracy of the results. The values that were used for these parameters are given below.

- Grid size,  $\Delta x = \Delta y$ .

A grid size of 45 m has been selected. 45 m is exactly the distance between the piers of the barrier.

- Time step,  $\Delta t$

A time step of 15 s is used to obtain an accurate computed flow pattern.

- Eddy viscosity coefficient,  $v_t$

For an correct reproduction of the velocity gradients and eddies downstream of the barrier the value of  $v_t$  had to be  $2 \text{ m}^2/\text{s}$  has been used. The numerical viscosity is negligible compared with this value of  $v_t$ .

- Roughness parameter,  $C$

A Chézy value is used which corresponds to a fixed value of the Manning coefficient  $n = 0.0262 \text{ m}^{1/3}/\text{s}$ . The value of the roughness parameters is of minor importance in the small detail models. It determines the overall tidal motion.

- Discharge coefficient,  $\mu$

The discharge coefficients are derived from steady state flume tests

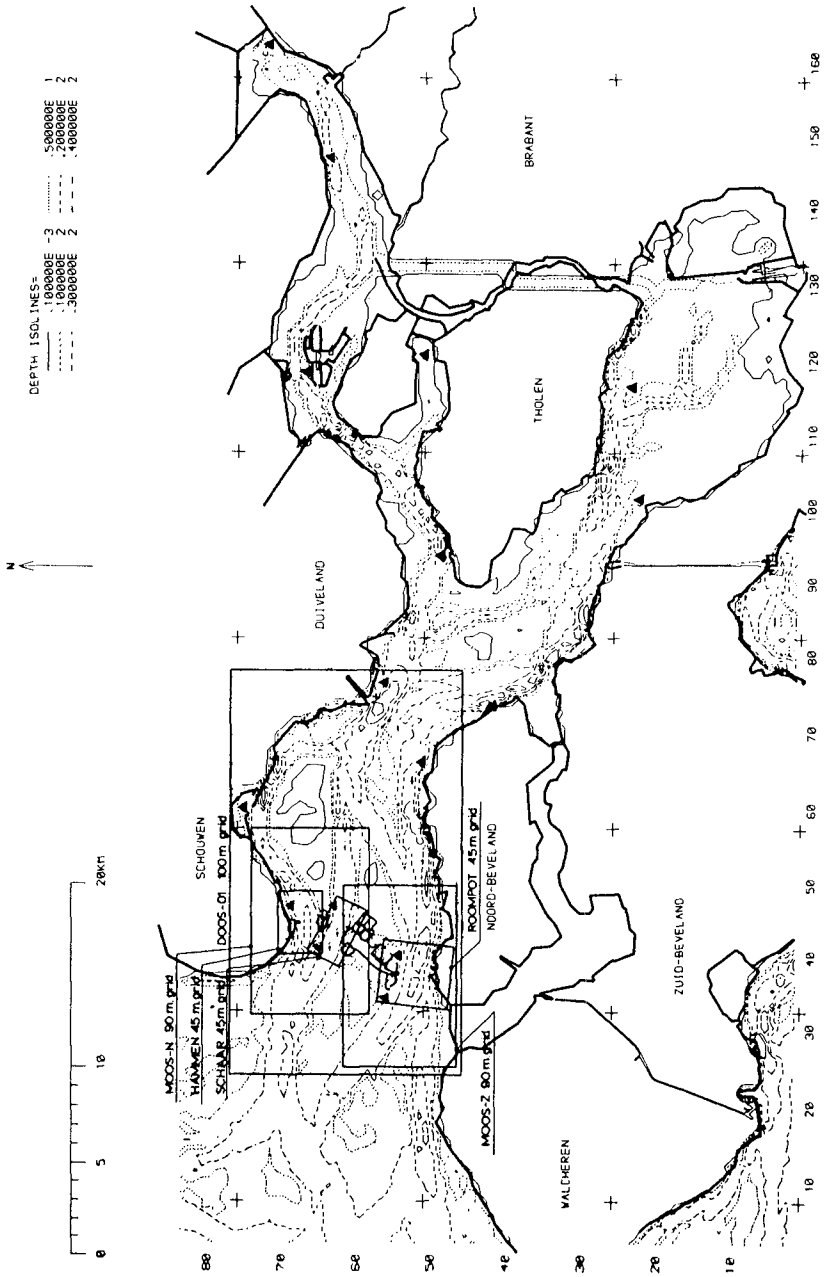


Figure 4. Lay-Out of the Numerical Models

for a 45 m section; 45 m is the distance between the piers. The coefficients were determined for both flow directions for a number of different construction stages and locations.

### Results

The construction of the barrier in the Eastern Scheldt is accompanied by an extensive hydraulic measurement campaign.

The hydraulically most interesting phase is the installation of the sill beams, Figure 2. These beams reduce the flow area between the piers abruptly. This causes an abrupt change of the flow pattern. Installation of the sill beams was a crucial phase for:

- the floating construction equipment
- morphological changes
- the stability of the bed protection near the barrier
- the development of scour holes at the boundaries of the bed protection

For 15 construction stages extensive field data are available. These data consist of waterlevels, head differences, discharges, flow velocities and flow directions upstream, downstream and at the site of the barrier. Special equipment was developed to obtain these field data.

The tidal flow has been computed by the WAQUA system for all these construction stages and was compared with the observed flow.

General conclusions on the three numerical methods used to introduce energy losses at the barrier site are:

- Method 1: Substitution of the long wave equation by a barrier equation.

The flow pattern downstream the barrier, which is with this method an internal boundary in the model, is disturbed. (compare Figure 11 with Figure 12) The computed total discharge and head difference agree well with observations.

- Method 2: Adapted fixed roughness.

The downstream flow pattern is correct; the barrier is no longer an internal boundary in the model. A disadvantage is the general approximation of the resistance and, because an averaged roughness is used, it is not possible to account for the influence of different flow directions and different flow conditions. This results in a less accurate reproduction of the discharge and the head difference than Method 1.

- Method 3: Dynamically adapted roughness.

This proves to be the best solution and the disadvantages of Method 1 as well as of Method 2 are avoided.

For this study the results of a scale model of the mouth of the Eastern Scheldt are available for comparison. This model is an undistorted steady state model with scale 1:80 of approximately the same area as the 45 m grid size numerical detail models. The indications are that the depth-averaged velocities computed with Method 3 agree as well with field data as depth-averaged velocities obtained from the scale model.

The results of the computations are discussed below in more detail for

two situations, see Figure 5:

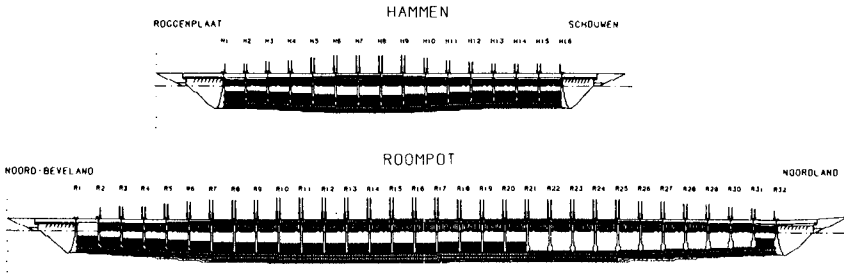


Figure 5. Geometry of the Barrier Under Construction in the Roompot and the Hammen.

- The Roompot: a situation in which 21 of the 31 sill beams have been installed. Ebb flow.
- The Hammen: a situation in which all 15 sill beams have been installed. Flood flow.

In these situations the flow is dominated by two-dimensional effects:

- The Roompot: At the transition between the rubble sill and the concrete sill beams there is a sharp discontinuity in the barrier: In the flow opening and in the discharge coefficient. Downstream this discontinuity a mixing zone develops with a sharp velocity gradient.
- The Hammen: Downstream of the barrier a large eddy is formed.

The results presented below have been computed with Method 2: Adapted fixed roughness. Except for one example which shows the effect of Method 1: Substitution of the long wave equation by a barrier equation. On basis of these results it was decided to develop and program Method 3: Dynamically adapted roughness. The initial tests showed that Method 3 is very promising.

The results for both the Roompot and Hammen flow situations are presented in Figures 6 through 13:

- The computed flow pattern in the Roompot has been plotted in Figure 6 for maximum ebb flow.
- In Figure 7 the observed and computed transport rate in the Roompot are given for both ebb flow and flood flow.
- The observed and computed flow velocities and flow directions at 350 m upstream and 630 m downstream of the barrier are presented in Figures 8 and 9 (maximum ebb flow).
- The transport rate per gate opening has also been plotted in Figure 8.
- The transport rate in the Hammen is presented in Figure 10
- In Figure 11 the computed flow pattern in the Hammen during maximum flood flow has been plotted.
- The flow pattern in the Hammen computed with Method 1 (barrier equation substituted) has been plotted in Figure 12; to be compared with Figure 11.

- Figure 13 finally gives the observed and computed velocities at 400 m upstream and 630 m downstream of the barrier and the transport rate per barrier gate (maximum flood flow). Additionally to the field data and computed velocities the observed flow velocities in the scale model are given 630 m downstream of the barrier.

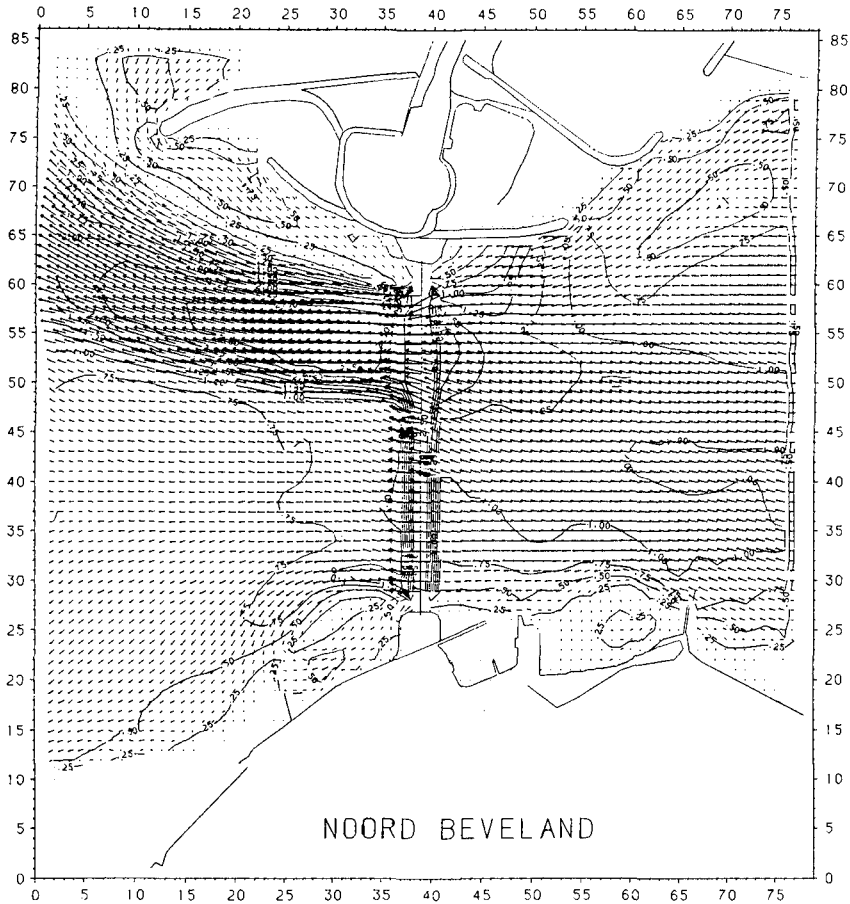


Figure 6. Roopot, Flow Pattern Maximum Ebb Flow.

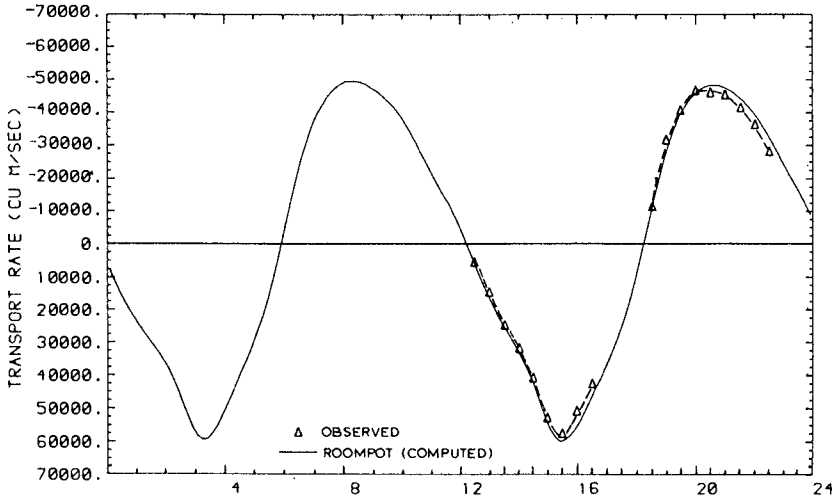


Figure 7. Roompot, Transport Rate.

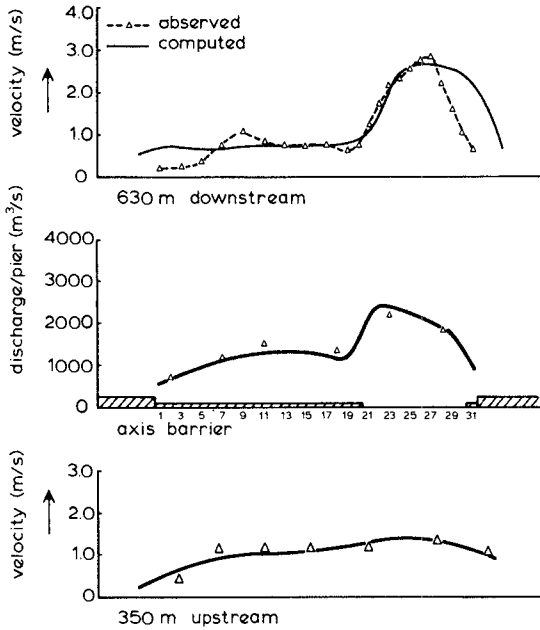


Figure 8. Roompot, Flow Velocities Maximum Ebb Flow.

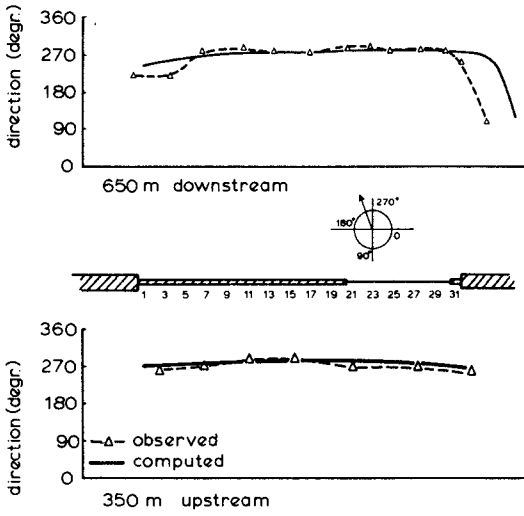


Figure 9. Roompot, Flow Directions Maximum Ebb Flow.

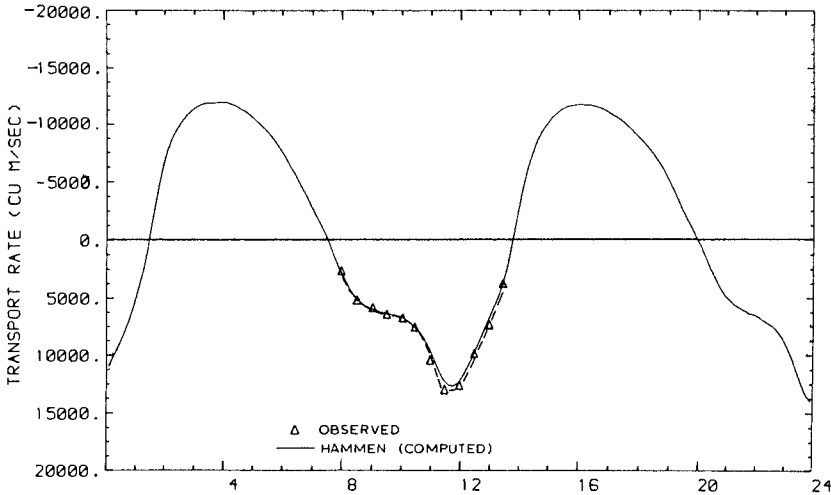


Figure 10. Hammen, Transport Rate.

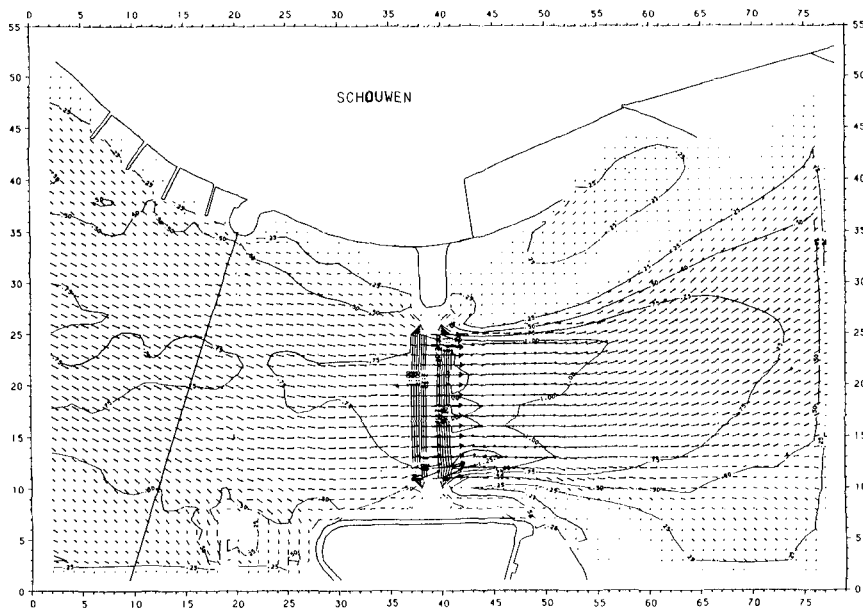


Figure 11. Hammen, Flow Pattern Maximum Flood Flow (Method 2).

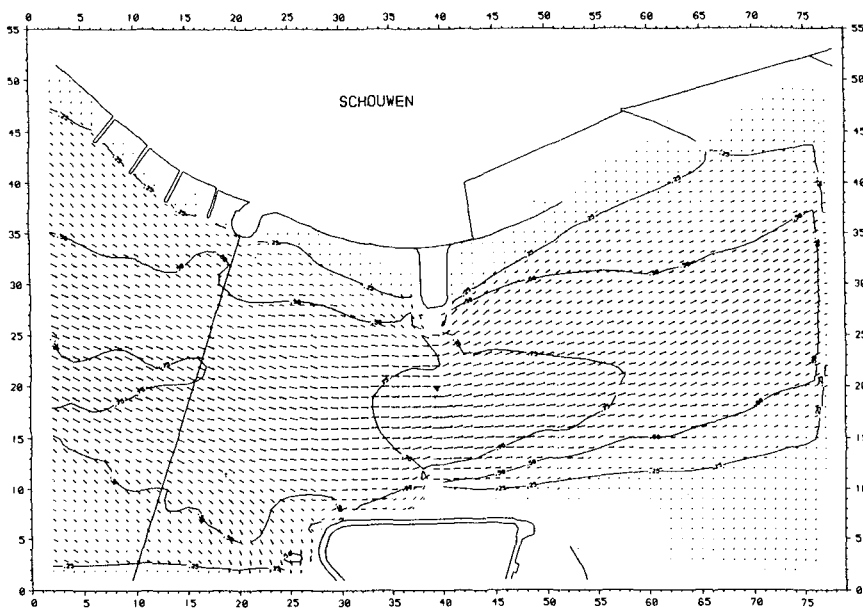


Figure 12. Hammen, Flow Pattern Maximum Flood Flow (Method 1).

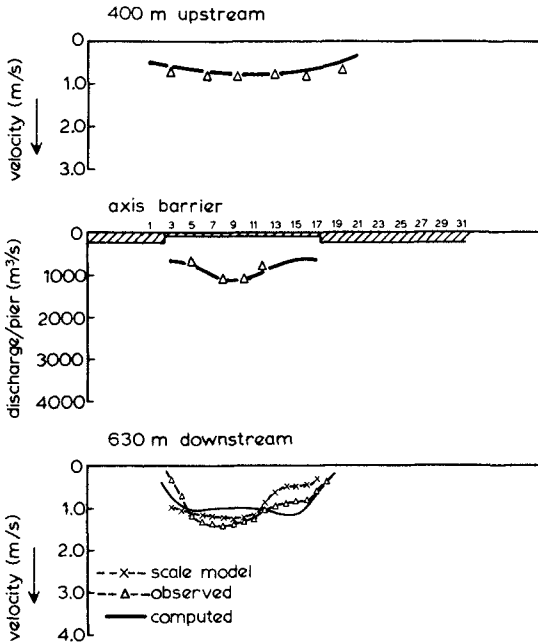


Figure 13. Hammen, Flow Velocities Maximum Flood Flow.

#### Conclusions

Comparison of the results computed by the WAQUA system with the field data shows that in general the agreement between WAQUA and the field data is good:

- Computed transport rates agree well with field data
- The agreement between the computed flow patterns and the field data is very good upstream of the barrier and at the site of the barrier
- Downstream the barrier the agreement between the computations and field data is acceptable. The computed maximum velocities and the steepness of the velocity gradients are correct. The locations where these occur however are not accurate. For engineering applications, for example calculation of the stability of bed protection or calculations of scour holes, this difference is acceptable.

The quality of the depth-averaged flow pattern computed by WAQUA is as accurate as that obtained from a large physical scale model. The method to deal with the energy losses at the barrier site greatly influenced the quality of the results.

This paper demonstrates that a method based on a local adaptation of the roughness is an accurate way of dealing with these local energy losses.

## References

1. Blik, A.J., Klatter, H.E., Koster, J.L.M., van der Meulen, T. "Short Cut Channels in Tidal Estuaries", proceedings, Third International Symposium on River Sedimentation, Jackson, Mississippi, USA, 1986.
2. Leendertse, J.J. "A Water Quality Simulation Model for Well Mixed Estuaries and Coastal Seas", Principles of Computation, Vol. I, RM-6230-RC, Rand. Corp., Santa Monica, USA, 1970.
3. Stelling, G.S., "On the Construction of Computational Methods for Shallow Water Flow Problems", Ph.D. thesis Delft University of Technology, Delft, The Netherlands, 1983. Also appeared as Rijks-waterstaat Communications, No. 35, The Hague, The Netherlands, 1984.
4. Stelling, G.S., Wiersma, A.K., Willemsse, J.B.T.M., "Practical Aspects of Accurate Tidal Computations", Journal of Hydraulic Engineering, Vol 112, No. 9, September 1986.